

Article

Rare Element Enrichment in Lithium Pegmatite Exomorphic Halos and Implications for Exploration: Evidence from the Leinster Albite-Spodumene Pegmatite Belt, Southeast Ireland

Renata Barros ^{1,2,*}, David Kaeter ^{1,3}, Julian F. Menuge ^{1,3} , Thomas Fegan ⁴ and John Harrop ⁴

¹ School of Earth Sciences, University College Dublin, Belfield, D04 V1W8 Dublin, Ireland; david.kaeter@ucdconnect.ie (D.K.); j.f.menuge@ucd.ie (J.F.M.)

² Geological Survey of Belgium, Royal Belgian Institute of Natural Sciences, 1000 Brussels, Belgium

³ iCRAG, University College Dublin, Belfield, D04 V1W8 Dublin, Ireland

⁴ Blackstairs Lithium Limited, The Black Church, St. Mary's Place, D07 P4AX Dublin, Ireland; fegan.thomas@gmail.com (T.F.); jcharrop@gmail.com (J.H.)

* Correspondence: renata.barros@ucdconnect.ie

Abstract: Pegmatitic deposits of critical metals (e.g., Li, Ta, Be) are becoming increasingly significant, with growing interest in understanding metal enrichment processes and potential vectors to aid the discovery of new resources. In southeast Ireland, the Leinster pegmatite belt comprises several largely concealed Li-Cs-Ta albite-spodumene-type pegmatites. We carried out detailed mineralogical characterization and whole-rock geochemical analyses of six drill cores intersecting pegmatite bodies and their country rocks. Exomorphic halos 2–6 m thick, enriched in Li, Rb, Be, B, Cs, Sn and Ta, are identified in both mica schists and granitic rocks adjacent to spodumene pegmatites. Metasomatism in wall rocks visible to the naked eye is restricted to a few tens of centimeters, suggesting country rock permeability plays a key role in the dispersion of these fluids. We propose that halos result from the discharge of rare element-rich residual fluids exsolved near the end of pegmatite crystallization. Halo geochemistry reflects the internal evolution of the crystallizing pegmatite system, with residual fluid rich in incompatible elements accumulated by geochemical fractionation (Be, B, Cs, Sn, Ta) and by auto-metasomatic resorption of spodumene and K-feldspar (Li, Rb). The possibility of identifying rare-element enrichment trends by analysis of bedrock, stream sediments and soils brings opportunities for mineral exploration strategies in Ireland and for similar albite-spodumene pegmatites worldwide.

Keywords: Leinster pegmatite belt; spodumene pegmatite; exomorphic halo; geochemical exploration



Citation: Barros, R.; Kaeter, D.; Menuge, J.F.; Fegan, T.; Harrop, J. Rare Element Enrichment in Lithium Pegmatite Exomorphic Halos and Implications for Exploration: Evidence from the Leinster Albite-Spodumene Pegmatite Belt, Southeast Ireland. *Minerals* **2022**, *12*, 981. <https://doi.org/10.3390/min12080981>

Academic Editors: Axel Müller and Encarnación Roda-Robles

Received: 31 May 2022

Accepted: 28 July 2022

Published: 1 August 2022

Publisher's Note: MDPI stays neutral with regard to jurisdictional claims in published maps and institutional affiliations.



Copyright: © 2022 by the authors. Licensee MDPI, Basel, Switzerland. This article is an open access article distributed under the terms and conditions of the Creative Commons Attribution (CC BY) license (<https://creativecommons.org/licenses/by/4.0/>).

1. Introduction

Pegmatites are typically very coarse-grained, usually small, igneous rock bodies. Granitic pegmatites, the commonest type, constitute economic sources of many industrial and critical minerals [1–3]. As industry develops a growing range of high-technology products containing rare elements, interest in understanding pegmatite petrogenesis and rare-metal enrichment grows accordingly. In this context, spodumene pegmatites are particularly significant due to their high concentrations of economically extractable Li and the presence of other metals used in high-technology applications, such as Ta and Sn. Global production of Li has increased about three times in the last five years to fulfill the increasing demand from the lithium-ion battery market, mostly towards the decarbonization of transport [4]. In Europe, Li was added to the Critical Raw Materials list in 2020 and there is a strong interest in expanding local production to reduce its criticality [5].

The relatively sudden upturn in interest in Li has exposed the incomplete geological understanding of Li-rich pegmatites. Key unresolved questions concern changes in magma or melt chemistry during crystallization and chemical interactions with country rocks during and after crystallization. Concerning the latter, it is well-known that rocks that host

different types of magmatic-related deposits undergo varying degrees of hydrothermal alteration, weakening away from the mineralized body [6]. Globally, such exomorphic halos (Li, Rb, Cs, Be, B, F, H₂O, Sn) are common in the country rocks hosting Li-rich pegmatites and their exploration potential is known [7–12], though their mineralogy and geochemistry have rarely been studied in detail in relation to pegmatite petrogenesis (e.g., [7,13,14]). The links between the development of exomorphic halos and the evolution of pegmatite crystallization are also poorly explored. The lack of detailed petrogenetic models for albite-spodumene pegmatites and their halos has greatly limited the scope of mineral exploration techniques for this pegmatite type, especially means by which the most prospective pegmatites in a swarm could be targeted.

In Leinster, southeast Ireland, a spodumene pegmatite belt has been known since the 1960s. It is virtually unexposed, but numerous concentrations of boulders have led to repeated mineral exploration interest. Since 1970, exploration drilling has demonstrated several spodumene pegmatites in the belt, which has its main bodies located along the eastern margin of the mainly ~400–420 Ma [15] S-type Leinster Batholith. Exploration has largely focused on known boulder accumulations and soil geochemical anomalies due to the lack of other effective exploration strategies.

Previously published mineralogical, petrographic and geochemical descriptions of Leinster pegmatites in general did not account for their interaction zones with wall rocks (e.g., [16,17]). Advances in the understanding of the internal processes and geochemical evolution in these pegmatites [18–20] now allow for better insight into the formation of exomorphic halos. Moreover, a recent and ongoing mineral exploration drilling campaign has provided an excellent opportunity for study.

In this paper, we set out a petrographic description and whole-rock geochemical analyses of six drill cores through spodumene pegmatite and immediate country rocks whose recovery is close to 100%. This information is supported by the logging of the drill core and previous work on outcrops and boulders in the field. Particular attention is paid to the nature of contacts between pegmatites and their country rocks. We qualitatively model the crystallization history of the intrusions and show that exomorphic halos that developed in wall rocks adjacent to the spodumene pegmatites are enriched in various rare elements of economic interest such as Li, Cs, Ta and Sn. We argue that exomorphic halos are formed at a late stage of the internal evolution of pegmatite bodies, contemporaneously, with the change from the crystallization of coarse early-primary minerals to fine-grained late-primary albitization. Both halo formation and albitization result from the expulsion of volatile and fluxing elements from the crystallizing pegmatite melt. Finally, we discuss the implications of our interpretations for mineral exploration.

2. Study Area

The study area is located in southeast Ireland within the Leinster Terrane (Figure 1), which is dominated by sedimentary rocks deposited between the Cambrian and Lower Ordovician in the Iapetus basin and deformed and affected by low-grade metamorphism during the Caledonian orogenic cycle resulting, ultimately, from the closure of the Iapetus Ocean [21–23]. The Ribband Group is the most dominant in the area and of special interest as these are immediate country rocks, usually in the hanging wall, of some Leinster pegmatites. The group consists of a thick succession of finely laminated mudstones deposited during the Lower Ordovician, with occurrences of coticule and andesite lava [24].

The largest of the granitic bodies in the Leinster Terrane is the Leinster Batholith, composed at least in part of sheeted intrusions of S-type two-mica granitic rocks [25–27]. It is mapped as four plutons of granite-granodiorite aligned with the NE–SW regional strike (Figure 1). The ascent and emplacement of magma batches that compose the Leinster Batholith is thought to have been facilitated by the East Carlow Deformation Zone (ECDZ), a 3 km wide dip-slip ductile deformation zone active from the Middle Ordovician to the late Carboniferous [24,28]. The largest and least exposed part of the Leinster Batholith is the Tullow Lowlands pluton, which hosts LCT pegmatites along its eastern margin within the ECDZ. It comprises equigranular and homogeneous granitic rocks, occasionally porphyritic with K-feldspar megacrysts, as well as foliated and sheeted margins with abundant granitic fingers within the adjacent schist, many of which remain undifferentiated in the local geological sequence [24,27]. Their compositions vary from monzogranite to granodiorite, with subordinate tonalite [16]. The heat provided by the emplacement of large volumes of Leinster and older Blackstairs granitic magmas has imposed a thermal aureole of contact metamorphism (up to 400 m wide) in the Ribband Group, turning regional greenschist facies metasediments into pelitic and psammitic schists, with subordinate amphibolites and chlorite schists of a volcanic origin [24]. The development of schistosity along with porphyroblasts of sillimanite, staurolite, garnet, andalusite and biotite indicate aureole temperatures above 500 °C [24,29].

The Leinster lithium pegmatite belt includes several mineralized (spodumene-bearing) and many simple (quartz-feldspar-muscovite ± garnet) granitic pegmatite bodies ranging from tens of cm to tens of m wide, with spodumene pegmatites known from at least ten localities along the eastern margin of the Leinster Batholith (Figure 1). Mineralized pegmatites are of the Li-Cs-Ta (LCT) albite-spodumene type [30] and host high concentrations of Li (estimated between 1.5–3% Li₂O) and economic potential for Ta and Sn. There appears to be no regional or district zonation of pegmatite composition relative to the margin of the Tullow Lowlands pluton. Occurrences are mostly within the ECDZ and thinner intrusions present complex interfingering relationships with their country rocks, which are primarily the Tullow Lowlands pluton and marginal granitic intrusions (Figure 2), but occasionally Ribband Group schists. Mineralized pegmatites typically have a mineral assemblage of 10–40% spodumene and varying quantities of K-feldspar, albite, quartz, muscovite and garnet, with accessory apatite, beryl, columbite-tantalite group minerals and sphalerite, among others [18–20]. They are usually unzoned bodies, but some thicker intrusions have quartz-rich cores. Primary megacrysts of spodumene and K-feldspar are often broken and may be parallel to the pegmatite contact surface near borders, which might indicate crystallization associated with deformation event(s) in the ECDZ or to internal stresses generated by pegmatite crystallization.

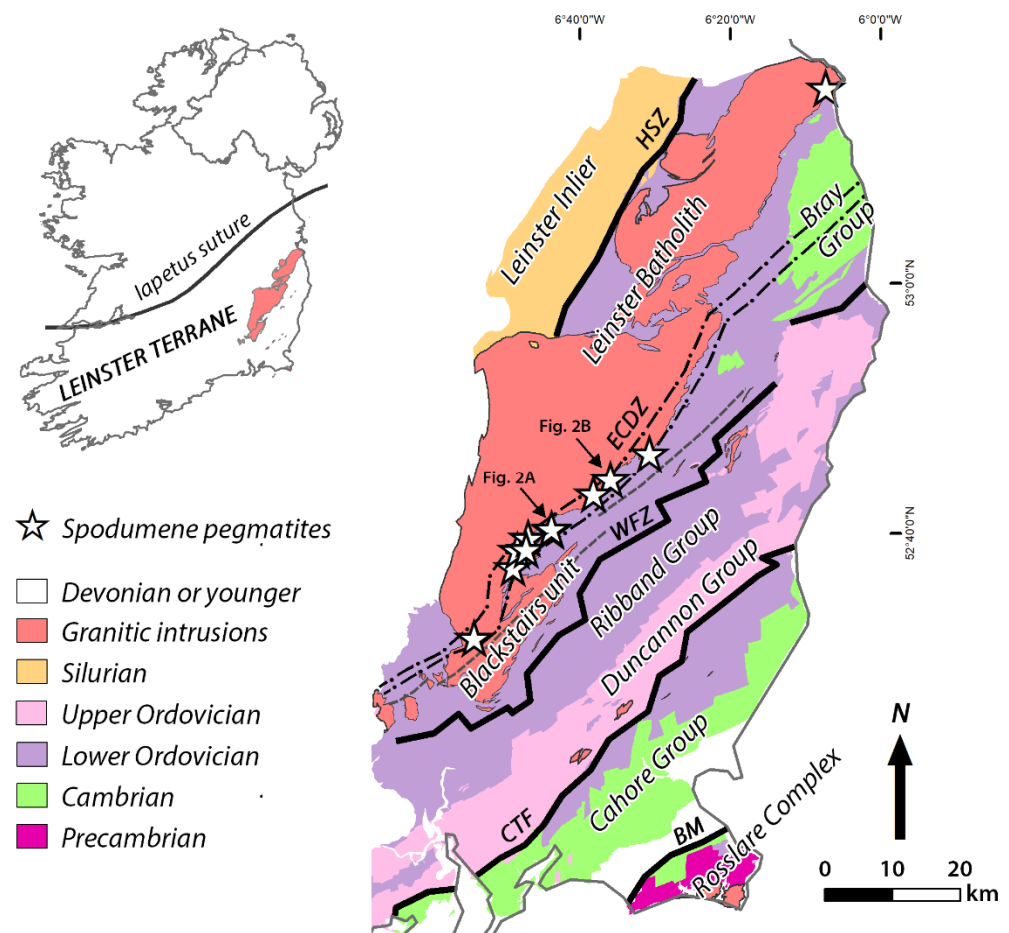


Figure 1. Simplified overview of the geology of the Leinster Terrane, south of the Iapetus suture, southeast Ireland. The Iapetus suture is according to [27]. The Leinster Batholith is shown in both overview (top left, inset) and the main map; major structures from the left: HSZ = Hollywood Shear Zone, ECDZ = East Carlow Deformation Zone [28]; WFZ = Wicklow Fault Zone [31]; CTF = Courtown–Tramore Fault [32]; BM = Ballycogly mylonites. Geological units from the 1:500,000 geological mapping shapefiles of Geological Survey Ireland.

3. Materials and Methods

The description of rock types and textures and samples collected to characterize pegmatite bodies and country rocks were mostly carried out from in situ occurrences intercepted by drill cores from the localities Aclare and Moylisha (Figure 2), part of the ongoing exploration campaign of Blackstairs Lithium Ltd. since 2011. Additional work was carried out on outcrops in the areas of Monaghanrim, Moylisha, Graiguenamanagh and Killiney Hill, as well as boulders located in Stranakelly, Moylisha, Monaghanrim and Aclare.

A detailed description was made of six drill cores of variable inclinations (45° to vertical) with virtually complete recovery that intercepted shallow-dipping pegmatites approximately perpendicular to contacts with country rocks, three from Aclare (6 cm diameter) and three from Moylisha (4 cm diameter), that represent the bedrock occurrences most enriched in spodumene (Figure 2).

Ninety-three representative samples were chosen for microscopic characterization with a Nikon Eclipse LV100POL polarizing optical microscope, using transmitted light, and a Hitachi TM-1000 scanning electron microscope in the School of Earth Sciences, University College Dublin, Ireland. Backscattered electron (BSE) images were obtained during electron microprobe work [18] using the Cameca SX 100 electron microprobe at the

Joint Laboratory of Electron Microscopy and Microanalysis of the Department of Geological Sciences, Masaryk University, Brno, Czech Republic.

Whole-rock geochemical analyses were obtained for pegmatites, hanging wall and footwall (country rocks to pegmatite intrusions) as part of the exploration campaign. The six drill cores were each split in half and divided into lithologically homogeneous parts, between 7 cm and 3.05 m long, resulting in 272 samples varying between 200 g and 2 kg, depending on interval length. These samples were then crushed, decomposed by four-acid digestion and analyzed for 48 elements by ICP-MS by ALS Minerals (Loughrea, Co. Galway, Ireland). Routine practices were used to ensure data quality control: sample duplicates (1 in every 20 samples), homogeneous quartz pebbles (1/40) and certified standards (1/20). Results showed reproducibility between duplicates within 15% for most elements and no contamination problems. Detection limits for the elements analyzed ranged between 0.02 and 100 ppm.

The volumes of the samples analyzed are considered representative to estimate the whole-rock geochemistry of pegmatite wall rocks and Leinster pegmatites, considering their typical grain size around 2 cm and negligible variations in pegmatite mineralogy among drill cores, boulders and outcrops of the same locality. It is assumed that the drill core samples are representative of the pegmatite bodies from border to border and that each pegmatite body crystallized from a single batch of magma [33].

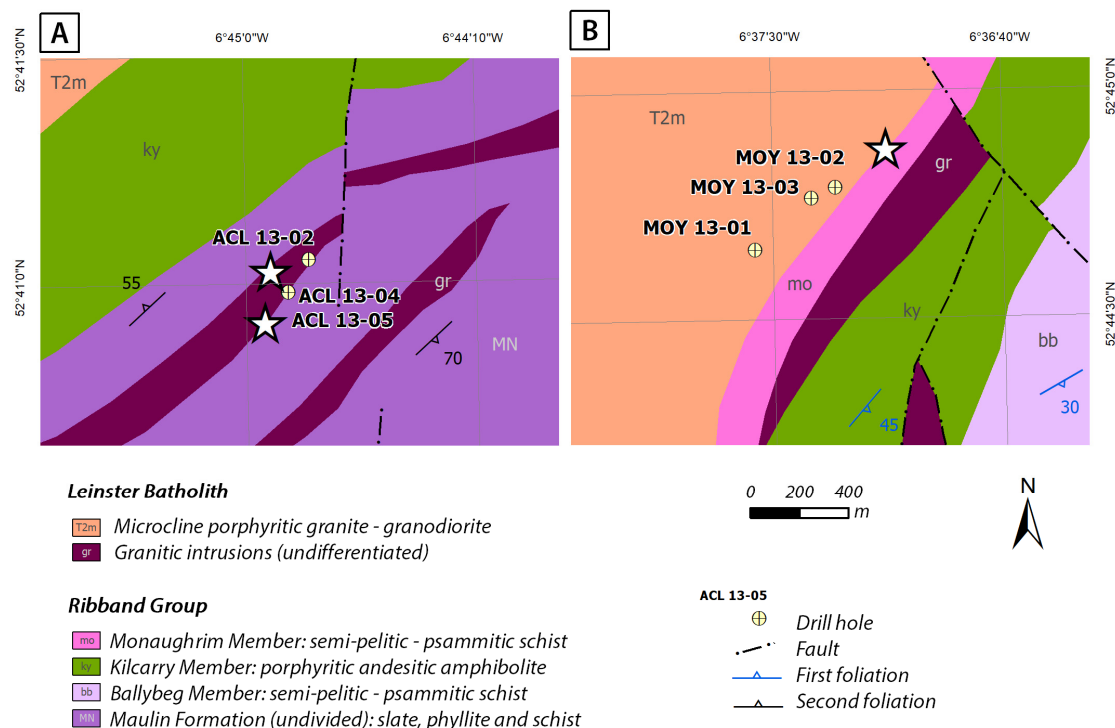


Figure 2. Location of drill collars studied in (A) Aclare and (B) Moylisha. Both areas represented are within the ECDZ. Geological units from the 1:500,000 geological mapping shapefiles of Geological Survey Ireland. White stars as in Figure 1.

4. Results

4.1. Mineralogical and Petrographic Features

A full description of the pegmatites and wall rocks is provided by [18] and summarized below. Spodumene pegmatites in Leinster are unzoned with spodumene present from contacts to the center of the intrusion or weakly zoned with a quartz core. Intrusions are mostly dominated by the early primary assemblage composed of medium-to-coarse-grained spodumene, quartz, K-feldspar, albite, muscovite, garnet (Figure 3A) and a variety of accessory phases, such as Mn-bearing fluorapatite, sphalerite and cassiterite. Spodumene

occurs as large subhedral prisms or laths from a few mm to tens of cm. The lack of intrusion scale of the geochemical and mineralogical zonation suggests early-stage Li saturation in the pegmatite melts [18].

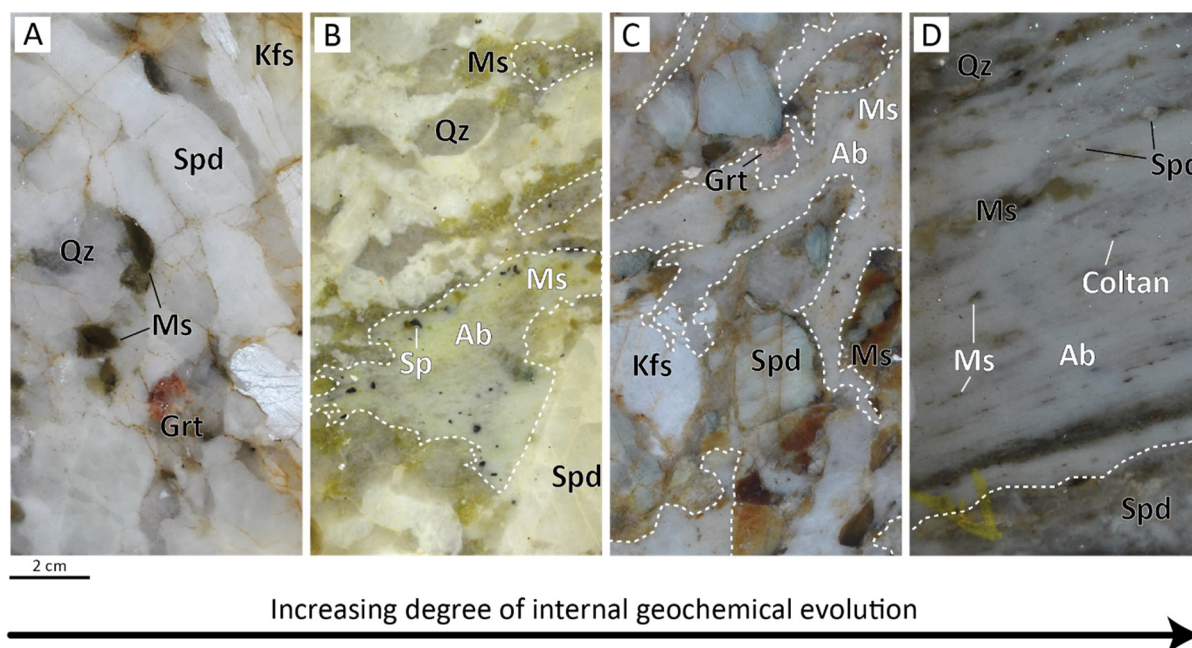


Figure 3. Representative textures indicating the internal evolution of spodumene pegmatites in Aclare; the same evolution is observed in Moylisha. Mineral abbreviations: Ab = albitite, Coltan = columbite-tantalite group minerals, Grt = garnet, Kfs = K-feldspar, Ms = muscovite, Qz = quartz, Sp = sphalerite, Spd = spodumene. (A) Typical early primary assemblage with no albitization. (B) Early primary assemblage with patches of late primary albitite. (C) Interconnected albitite patches with visible alteration of early primary assemblage. (D) Predominant late primary albitite with relics of spodumene, quartz and muscovite. Extent of albitization is represented by white dashed lines. Scale bar is valid for all images.

The volume of fine-grained albitite, common in spodumene pegmatites, varies throughout intrusions, from isolated to interconnected patches (Figure 3B,C) and occasionally in intervals of tens of cm dominated by the fine-grained assemblage (Figure 3D). Albitization tends to be stronger downwards across spodumene pegmatite intersections. Albitite is recognized as a replacive late primary mineral assemblage at the final stages of pegmatite crystallization [18,19], as it both overgrows and partially replaces the primary minerals of the spodumene intervals. It consists of albitite crystals (~90%), often aligned where they occur in larger volumes, with minor muscovite and accessory garnet, apatite, beryl, cassiterite and columbite-group minerals. Variable alterations of spodumene to fine-grained mica and the resorption of K-feldspar are frequent and often only relics or pseudomorphs can be observed (Figure 3C,D). Large albitized spodumene and F-rich apatite crystals often result in a vermicular habit, though elsewhere, only the rims of these crystals are consumed. Particularly in Moylisha, interstitial and fracture-filling lithiophilite and polyolithionite rims in muscovite are common in the albitite.

The hanging wall of the uppermost Aclare spodumene pegmatite is the Ribband Group's Maulin Formation (Figure 2) consisting of garnet, staurolite and andalusite-bearing mica schists. A lens of undifferentiated foliated granodiorite forms the footwall of the uppermost intersections and fully encloses deeper Aclare pegmatites (Figure 2). Moylisha pegmatites are hosted in the margin of the Tullow Lowlands pluton (Figure 2), characterized by porphyritic granodiorite. Contacts with wall rocks are typically sharp and vary from irregular to subparallel to the regional foliation [18]. Spodumene pegmatite exocontacts in all country rock types are characterized by visibly altered zones containing a higher

concentration of mafic minerals; the thickness of these zones varies from 2 to 20 cm (Figure 4).

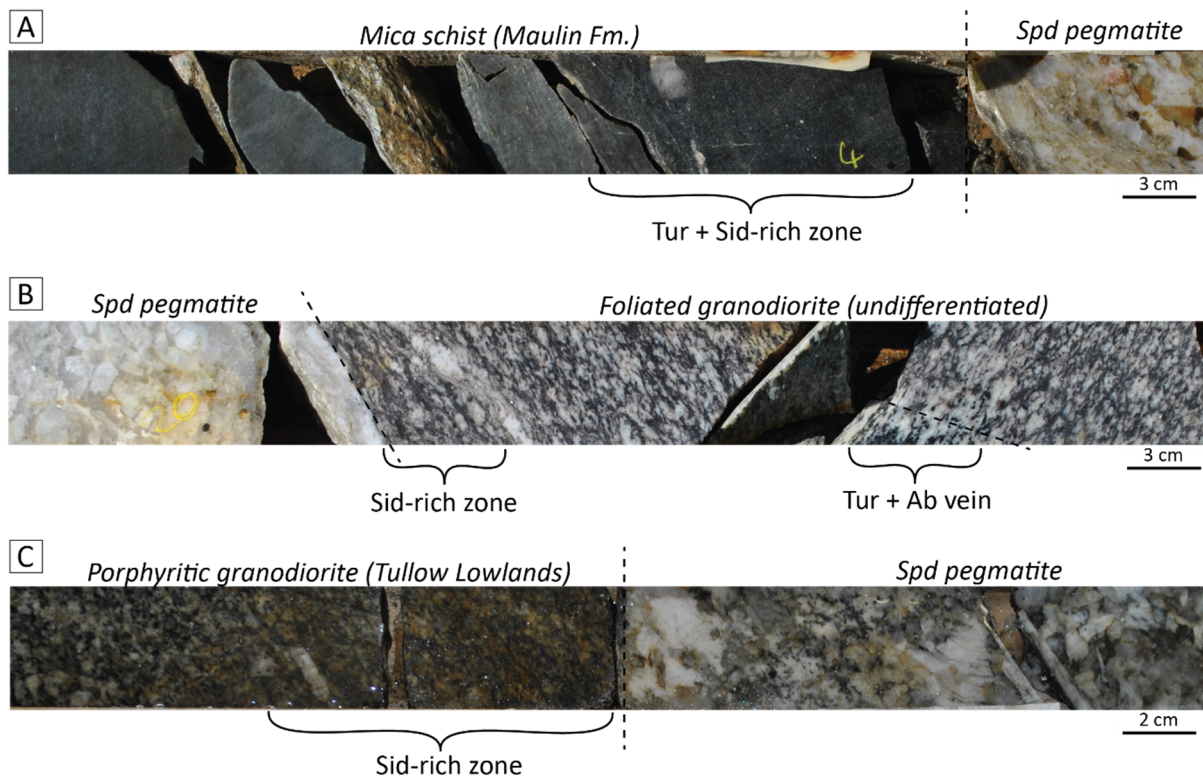


Figure 4. Exocontacts of spodumene pegmatites in the three country rock types. Mineral abbreviations: Ab = albite, Sid = siderophyllite, Spd: spodumene, Tur = tourmaline. (A) Hanging wall mica schist with a 15 cm zone of tourmaline and siderophyllite enrichment just above the spodumene pegmatite top contact, drill hole ACL 13-02. (B) Footwall foliated granodiorite with 5 cm zone enriched in siderophyllite adjacent to spodumene pegmatite bottom contact; note tourmaline-rich vein further from the contact, drill hole ACL 13-02. (C) Hanging wall porphyritic granodiorite with 10 cm zone enriched in siderophyllite just above spodumene pegmatite top contact, drill hole MOY 13-03.

Maulin Formation mica schists are dominated by bands of biotite (commonly altered to chlorite), muscovite and quartz, commonly with porphyroblasts of staurolite, garnet and andalusite (e.g., Figure 5A). Within the spodumene pegmatite exocontact (Figure 4A), the schist is mainly composed of light pink siderophyllite, pleochroic brown tourmaline (ranging between schorl and dravite) with darker rims, quartz and accessories including apatite, beryl (Figure 5B) and ilmenite. The foliated granodiorite has its foliation defined by aligned micas and quartz elongation surrounding oligoclase phenocrysts (>1 cm) (Figure 5C). The Aclare spodumene pegmatite exocontact in granodiorite is less pronounced than in schist (Figure 4B); medium-grained (1 to 2 mm) radiating tourmaline “poikiloblasts” (Figure 5D) and light red siderophyllite are present. The porphyritic granodiorite has abundant microcline megacrysts that may carry fine-grained oligoclase inclusions and occasional inclusions of biotite and myrmekite. In Moylisha, this rock may be foliated, with preserved K-feldspar megacrysts (Figure 5E). The Moylisha spodumene pegmatite exocontact is also less pronounced than in schist (Figure 4C), notably characterized by the presence of tourmaline (Figure 5F).

4.2. Whole-Rock Geochemistry

Leinster pegmatites have complex textures (e.g., Figure 3) and variable compositions within sampled intervals, which brings challenges for whole-rock geochemical characteri-

zation. Based on previous work [16,18,33], it is estimated that the main components, Si and Al, show similar variations between non-albitized and albitized spodumene pegmatites, with SiO₂ between 67 and 73 wt.% and Al₂O₃ between 17 and 22.9 wt.%; Fe and Li are major elements in spodumene pegmatites (up to 3.84 wt.% Fe₂O₃ and 4.28 wt.% Li₂O), but much less abundant in albitite (<0.3 wt.% Fe₂O₃ and <0.01 wt.% Li₂O); Na is more abundant in albitite (8.53–11.56 wt.%) than in spodumene pegmatite (1–3.2 wt.% NaO).

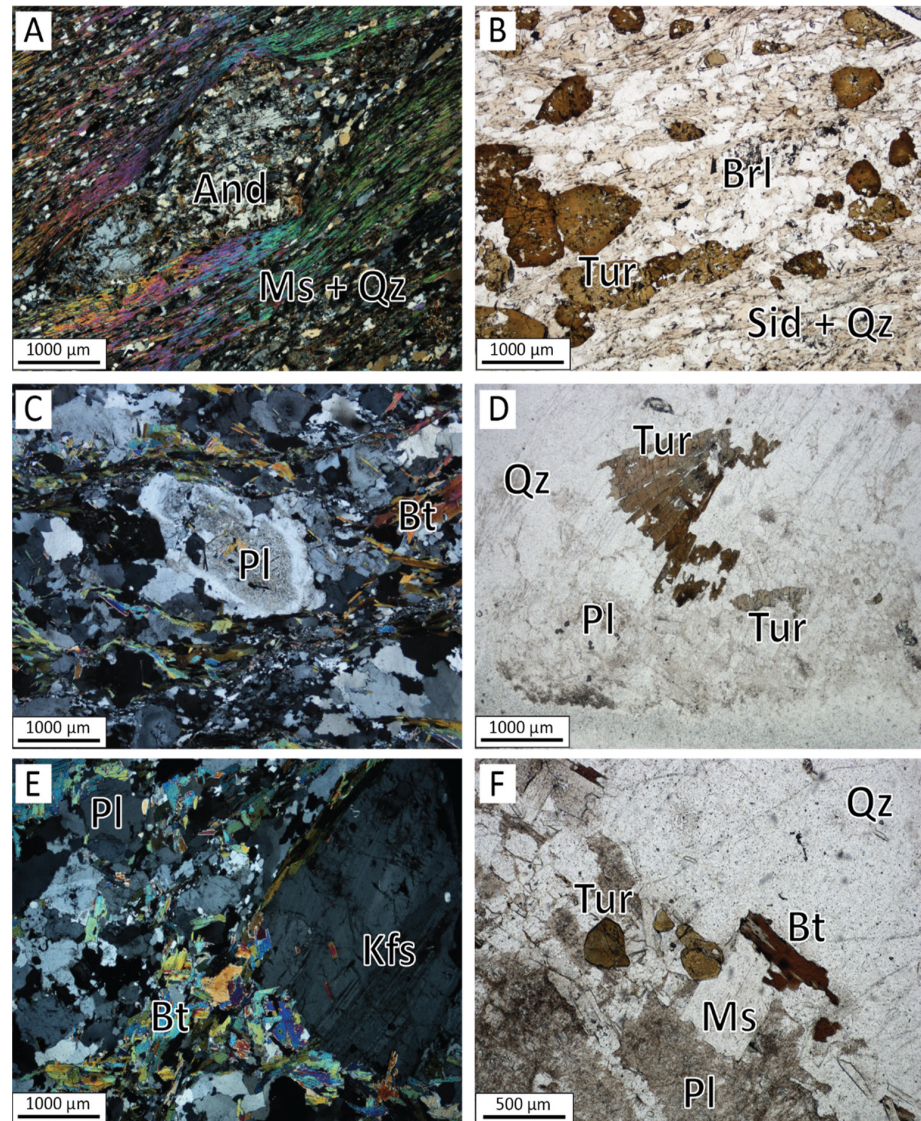


Figure 5. Mineralogy and textures in wall rocks. Mineral abbreviations: And = andalusite, Brl = beryl, Bt = biotite, Kfs = K-feldspar, Ms = muscovite, Pl = plagioclase, Qz = quartz, Sid = siderophyllite, Tur = tourmaline; samples from drill holes in parentheses. (A) Inclusion-rich andalusite porphyroblasts enveloped by aligned muscovite in mica schist (ACL 13-02). (B) Medium-grained light brown tourmaline crystals with dark brown rims within light pink siderophyllite, beryl and quartz in spodumene pegmatite exocontact in mica schist (ACL 13-02), 2 cm away from the contact with spodumene pegmatite. (C) Zoned plagioclase megacryst with inclusion-rich core and clear rim with irregular borders, within aligned biotite and muscovite crystals in foliated granodiorite (ACL 13-04). (D) Radiating tourmaline “poikiloblast” adjacent to quartz and zoned plagioclase in footwall granodiorite exocontact to spodumene pegmatite (ACL 13-04), 2.5 cm away from the contact with spodumene pegmatite. (E) Microcline megacryst in porphyritic granodiorite (MOY 13-03). (F) Tourmaline crystals in spodumene pegmatite exocontact in porphyritic granodiorite (MOY 13-03), 3 cm away from the contact with spodumene pegmatite.

Whole-rock concentrations for a series of relevant major and mostly trace elements in Aclare and Moylisha pegmatite and country rock samples are presented as Supplementary Table S1 and summarized in Table 1. In Aclare drill cores (Figure 6A–C), foliated granodiorite and mica schist have concentrations within a factor of twenty when compared to the upper continental crust (UCC) [34]. In the foliated granodiorite, enrichment in Li, Cs, Sn, Be, U and Pb and depletion in Ni, Hf and Zr is observed, while the schist is enriched in Li, Cs, Sn, Zn, Mn and Pb and depleted in Sr, Na and Ca. The samples of both rock types up to 1.5 m away from spodumene pegmatites contacts contain 10 to 200 times higher Li, Cs, Sn, Rb and Be, and lesser Ta enrichment, compared to UCC. In schist, enrichment in Zn and Pb is also observed in the halo. Li and Cs enrichment in schist may extend beyond the sampling limit of 6 m above the spodumene pegmatite contact.

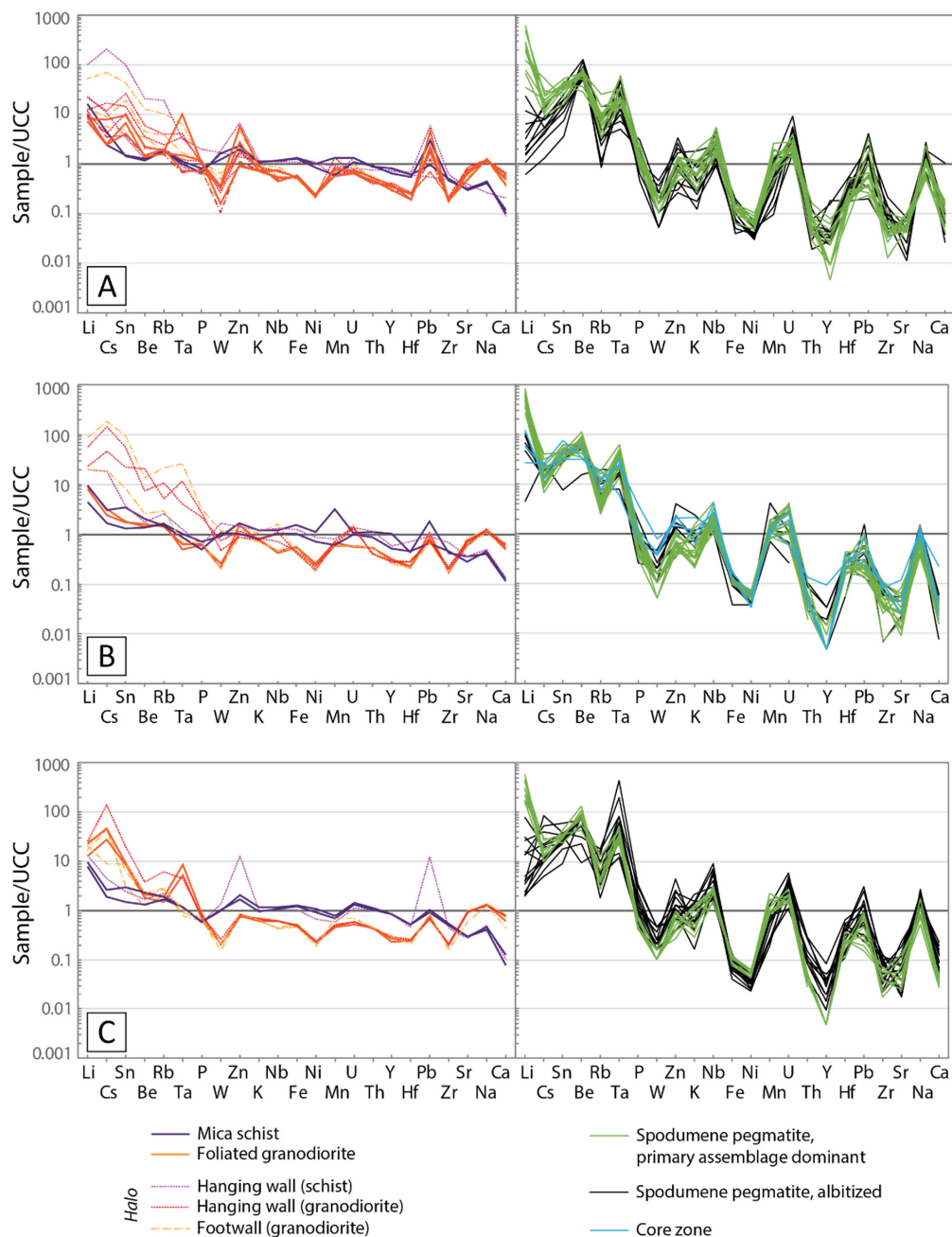


Figure 6. Whole-rock concentrations of elements of interest normalized against the upper continental crust (UCC; values from [34]) for the Aclare drill cores (A) ACL 13-02, (B) ACL 13-04 and (C) ACL 13-05.

Table 1. Summary of whole-rock analyses of pegmatites and country rocks.

Aclare															
				Mica Schist (n = 10)			Foliated Granodiorite (n = 28)			Spodumene Pegmatite, Primary Assemblage (n = 43)			Albitized Spodumene Pegmatite (n = 30)		
				mean	min	max	mean	min	max	mean	min	max	mean	min	max
Al	wt. %	0.01	2%	8.42	7.11	9.65	7.69	7.28	8.34	7.02	6.26	7.95	6.62	4.28	8.14
Be	ppm	0.05	3%	7.3	2.4	43.1	10.8	2.6	42.9	142.1	60.6	284.0	143.1	20.0	271.0
Ca	wt. %	0.01	2%	0.31	0.20	0.53	1.44	0.69	2.09	0.15	0.04	0.57	0.30	0.02	2.67
Cs	ppm	0.05	4%	124.2	8.0	1000	247.1	11.6	1000	85.2	32.9	264.0	80.4	6.6	418.0
Fe	wt. %	0.01	1%	4.84	4.08	6.07	2.00	1.65	2.28	0.45	0.21	0.66	0.38	0.15	0.78
Hf	ppm	0.1	2%	2.9	2.3	3.7	1.3	1.0	1.6	1.3	0.3	3.0	1.7	0.3	3.4
K	wt. %	0.01	2%	2.52	1.88	2.79	1.85	1.42	3.17	1.64	0.49	4.89	1.96	0.29	5.58
Li	ppm	0.2	3%	514.2	105.0	2420	692.2	175.5	2870	8824	98.8	19,700	506.5	15.2	2470
Mn	ppm	5	2%	782	437	2480	538	358	1030	947	151	2100	643	77	3300
Mo	ppm	0.05	12%	2.7	1.4	4.0	0.7	0.5	0.9	0.1	0.1	0.1	0.1	0.1	0.1
Na	wt. %	0.01	1%	1.04	0.63	1.21	2.92	1.94	3.39	2.31	0.88	5.81	4.03	1.32	6.78
Nb	ppm	0.1	6%	13.6	12.1	15.4	7.8	5.1	19.2	31.3	12.7	80.5	30.5	11.1	109.5
Ni	ppm	0.2	8%	43.8	32.2	53.1	10.5	8.6	12.0	2.8	1.2	5.0	1.9	1.1	3.2
P	ppm	10	4%	502	330	1310	741	400	2050	690	210	2550	852	170	2310
Pb	ppm	0.5	6%	47.6	9.4	211.0	21.3	11.3	77.8	8.9	2.4	58.4	18.6	2.3	70.0
Rb	ppm	0.1	4%	299.4	121.0	1580	501.4	118.5	2240	623.7	208.0	2100	615.1	72.1	1590
Sc	ppm	0.1	3%	18.0	15.1	20.4	6.2	5.3	6.8	0.2	0.1	0.9	0.2	0.1	0.7
Sn	ppm	0.2	4%	25.4	2.7	208.0	50.8	3.6	225.0	81.3	34.2	158.5	54.2	7.7	123.0
Sr	ppm	0.2	2%	102.7	89.5	124.5	230.0	139.5	323.0	16.8	2.9	42.9	20.3	3.7	76.7
Ta	ppm	0.05	5%	1.16	0.80	2.91	3.89	0.44	23.30	29.80	5.43	55.10	42.54	4.64	402.0
Th	ppm	0.2	8%	10.3	7.9	12.0	4.8	4.0	5.9	0.6	0.2	3.1	0.9	0.2	3.1
Tl	ppm	0.02	2%	1.72	0.57	9.79	3.31	0.58	14.00	4.30	1.27	16.55	4.25	0.33	16.25
U	ppm	0.1	3%	3.2	2.2	3.9	2.1	1.4	4.2	6.1	1.6	13.5	8.1	0.7	25.5
W	ppm	0.1	3%	2.6	1.7	3.5	0.8	0.2	3.0	0.3	0.1	1.5	0.5	0.1	0.9
Y	ppm	0.1	7%	15.9	10.9	21.6	6.5	4.9	8.7	0.4	0.1	2.0	0.8	0.1	3.9
Zn	ppm	2	2%	221	70	862	98	51	372	55	18	163	101	18	303
Zr	ppm	0.5	5%	98.8	80.7	131.0	37.0	31.8	42.5	10.3	1.4	23.2	15.3	1.3	42.8

Moylisha															
				Porphyritic Granodiorite (n = 77)			Simple Pegmatite (n = 42)			Spodumene Pegmatite, Primary Assemblage (n = 19)			Albitized Spodumene Pegmatite (n = 23)		
				mean	min	max	mean	min	max	mean	min	max	mean	min	max
Al	wt. %	0.01	2%	7.49	6.68	10.5	6.95	4.32	10.2	6.72	6.14	7.61	6.12	0.89	7.47
Be	ppm	0.05	3%	13.5	4.5	103.0	48.9	4.5	285.0	153.0	95.1	218.0	126.8	1.6	262.0
Ca	wt. %	0.01	2%	1.19	0.71	1.54	0.39	0.11	1.42	0.10	0.05	0.30	0.13	0.01	0.31
Cs	ppm	0.05	4%	64.0	9.8	343.0	44.4	14.2	226.0	75.4	49.3	115.5	57.0	15.9	143.5
Fe	wt. %	0.01	1%	1.72	1.22	2.00	0.65	0.31	1.21	0.39	0.27	0.56	0.28	0.17	0.50
Hf	ppm	0.1	2%	2.9	1.9	4.7	1.5	0.2	10.0	2.1	0.9	4.1	2.1	0.2	4.8
K	wt. %	0.01	2%	2.90	1.54	4.67	3.18	1.58	5.00	2.28	0.82	3.82	2.23	0.64	4.95
Li	ppm	0.2	3%	608.4	287.0	2560	258.1	80.2	1540	5500	239.0	12,750	340.1	63.2	1390
Mn	ppm	5	2%	624	406	2530	916	159	5990	907	539	1340	681	44	1520
Mo	ppm	0.05	12%	0.6	0.1	14.4	0.8	0.1	10.4	0.1	0.1	0.3	0.3	0.1	1.5
Na	wt. %	0.01	1%	2.61	0.69	3.14	2.81	0.98	5.26	2.79	1.10	4.67	4.00	0.13	6.32
Nb	ppm	0.1	6%	8.9	5.8	59.2	12.5	4.5	48.1	27.9	10.7	72.6	37.0	3.3	119.5
Ni	ppm	0.2	8%	6.4	4.0	8.5	2.6	1.1	4.9	2.6	1.4	4.6	2.5	0.7	16.2
P	ppm	10	4%	961	540	7000	779	190	7240	526	270	1180	480	90	1580
Pb	ppm	0.5	6%	28.8	8.1	36.3	24.4	6.8	46.3	16.5	7.4	29.6	17.9	5.5	40.7
Rb	ppm	0.1	4%	321.6	175.5	1360	402.5	224.0	1400	657.5	255.0	1300	478.5	176.0	1270
Sc	ppm	0.1	3%	4.5	2.8	5.5	1.0	0.2	3.0	0.1	0.1	0.7	0.1	0.1	0.3
Sn	ppm	0.2	4%	34.9	5.5	430.0	56.9	18.2	395.0	61.6	36.1	78.3	28.6	1.9	45.1
Sr	ppm	0.2	2%	153.9	40.9	194.5	38.9	17.4	87.0	12.3	5.5	27.8	20.0	4.1	77.7
Ta	ppm	0.05	5%	2.28	0.65	40.40	7.29	1.28	89.00	26.48	9.06	85.90	37.91	0.88	99.50
Th	ppm	0.2	8%	11.4	6.5	14.4	3.3	0.4	26.0	2.3	0.9	4.1	2.9	0.2	7.5
Tl	ppm	0.02	2%	1.89	1.00	9.15	2.34	1.08	8.38	4.56	1.43	10.05	3.32	0.87	12.15
U	ppm	0.1	3%	4.9	1.8	15.6	6.5	0.8	25.6	6.3	1.5	16.8	5.8	1.7	10.5
W	ppm	0.1	3%	0.9	0.2	5.8	1.1	0.2	4.6	0.3	0.1	0.4	0.4	0.1	0.6
Y	ppm	0.1	7%	8.2	5.6	9.6	4.5	0.6	22.7	0.2	0.1	1.0	0.7	0.1	5.6
Zn	ppm	2	2%	91	56	301	46	14	215	79	32	144	65	4	125
Zr	ppm	0.5	5%	97.6	58.0	120.5	26.2	3.5	102.5	13.4	4.7	28.1	13.3	1.0	29.9

Bold = detection limits; italicized = mean relative standard deviation of analyses. Complete analyses in Supplementary Table S1.

At the same locality, spodumene-bearing intervals in pegmatites have up to 1000 times more Li, and around 100 times more Cs, Be, Sn, Ta and Rb, than country rocks. They are depleted in W, Fe, Ni, Th, Y, Sr and Ca, a signature common to albite-spodumene pegmatites elsewhere, e.g., [35–37]. There is a large variation in Li, Cs, Sn, Rb, Zn, K, Nb and Y concentrations among different pegmatite samples, which may primarily be explained by variations in the proportions of spodumene and K-feldspar (primary assemblage) and minor phases such as sphalerite and columbite-tantalite group minerals in albitite (late

primary assemblage). Samples dominated by the primary assemblage have the highest Li, mostly >100 times UCC; samples dominated by the late primary assemblage show enrichment in Be, Ta, Nb and Y, but a major depletion in Li, when compared to the primary assemblage (e.g., Figure 6C). The quartz-feldspar core zone of ACL 13-04 presents a similar trend to the albitite, with around 100 times less Li when compared to spodumene-bearing samples (Figure 6B).

In Moylisha drill cores (Figure 7A–C), the porphyritic granodiorite shows a similar pattern to the foliated granodiorite: enrichment of up to 30 times UCC in Li and Sn, up to 10 times UCC in Cs, Be, Rb, Ta and U, and a depletion down to 0.1 times UCC in W and Ni. Granodiorite adjacent to spodumene pegmatites, up to 2 m from contacts, shows Li, Cs, Ta, Sn, Be and Rb from 10 to 100 times UCC. Peaks of Be and Sn concentrations in granodiorite samples distant from spodumene pegmatites are also observed (e.g., Figure 7B) and could result from interactions with simple pegmatites.

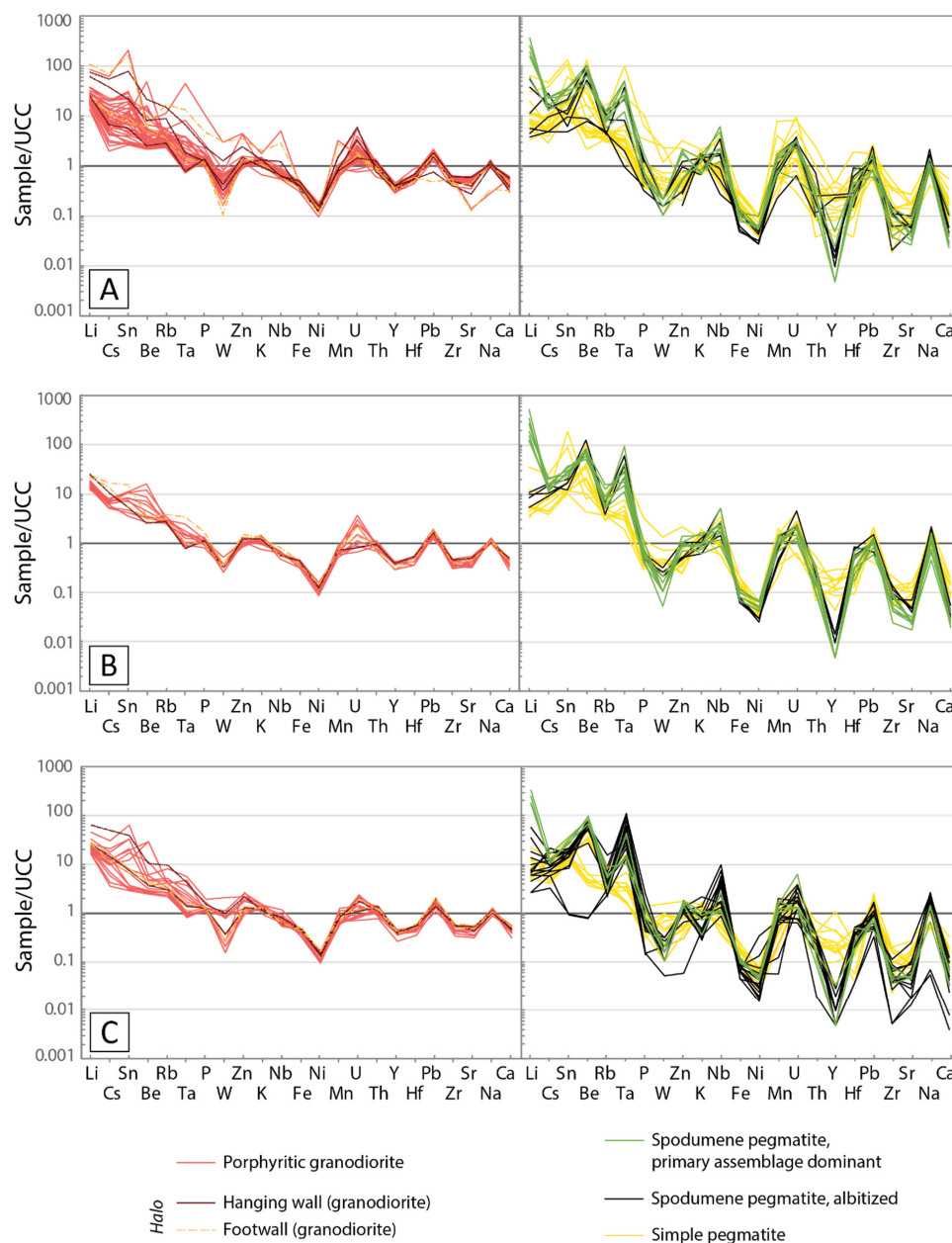


Figure 7. Whole-rock concentrations of elements of interest normalized against the upper continental crust (UCC; values from [34]) for the Moylisha drill cores (A) MOY 13-01, (B) MOY 13-02 and (C) MOY 13-03.

Moylisha spodumene pegmatites have up to 600 times more Li than UCC, along with elevated Be, Rb, Sn and Ta (up to 100 times UCC). As with Aclare spodumene pegmatites, they are depleted in W, Fe, Ni, Y, Zr, Sn and Ca. Albitized spodumene pegmatites are depleted in Li, but are not significantly different in Be, Ta, Nb and Sn concentrations, compared to unalbitized spodumene pegmatites. Simple pegmatites present some enrichment in Li, Be, Sn, Cs and Rb (around 3 to 10 times UCC, with Be reaching around 80 times UCC) and depletion in Sr, Ba, Hf, Zr and Y, similar to, but less pronounced than in, spodumene pegmatites.

4.3. Characterization of Exomorphic Halos

An enrichment in many incompatible elements is observed in spodumene pegmatite exocontacts in the three different country rock types. The elements Li, Cs, Ta, Rb, Be and Sn show the most noticeable exomorphic halo effect, with the most significant enrichments in country rocks closest to spodumene pegmatites, as shown in the drill core geochemical profiles (Figures 8 and 9). At Aclare (Figure 8), the mica schist shows pronounced concentration peaks of all these elements adjacent to the upper spodumene pegmatite contact, even where a direct contact was not preserved in the drill core (e.g., Figure 8B). This halo effect is also observed in the foliated granodiorite in the footwall, although the enrichment is less pronounced. Foliated granodiorite xenoliths in spodumene pegmatites, when present, show enrichment in Cs, Rb and Be compared to the parent granitic rock. At Moylisha (Figure 9), the halo effect is less pronounced, likely due to the less permeable and/or less reactive nature of the wall rock (porphyritic granodiorite) and the complexity imposed by several simple pegmatite intrusions; however, elevated Li and Cs concentrations in the hanging wall of spodumene pegmatites can be identified (most clearly in Figure 9C).

Table 2 presents an approximate quantification of the concentrations of elements lost from pegmatite magma to the exomorphic halo for Li, Be, Sn, Ta, Cs and Rb. This is estimated through data in Supplementary Table S1 following three steps: (1) identifying the lowest concentrations of the elements in wall rocks within 20 m of a contact with a spodumene pegmatite to obtain the approximate composition prior to pegmatite emplacement (or “background”); for the drill core MOY 13-01, the distance interval from contact considered was 10 m due to the small thickness of the spodumene pegmatites; (2) estimating the total weights of the elements in the halos by summing all the wall rock sampled intervals, weighted by interval length, with the background subtracted; (3) estimating the total pre-halo pegmatite weights by similarly summing all pegmatite and halo intervals. Differences in rock density are ignored, which provides a limitation to our calculations. However, the relative differences in specific gravity are unlikely to exceed 10% between spodumene pegmatite and mica schist and 5% between spodumene pegmatite and granite. The spreadsheet with calculations is presented as Supplementary Table S2. For these calculations, all simple pegmatite intervals in Moylisha drill cores, the boulder at the top of the drill core MOY 13-01 and the wall rock xenoliths in ACL 13-02 and ACL 13-05 were excluded, so that the calculation of the halo element inventories would be conservative; if simple pegmatites were intruded before spodumene pegmatites and lay within spodumene pegmatite halos, halo inventories would be slightly larger than calculated. Halo inventories may also be larger if halos were wider than covered by the analyzed samples, which were located within the maximum 20 m interval of available core length.

The estimated amount of Li lost from the spodumene pegmatites ranges from 2% to 12%; the smallest Li loss is observed in drill core ACL 13-04, which has the thickest zoned pegmatite, and the largest Li loss is observed in drill core MOY 13-03, where the intervals dominated by late primary albitite are most frequent (see Figure 7C). The estimated amounts of Be and Ta in the halos also represent no more than 7% of the pre-halo pegmatite inventory. Larger proportions of Sn, Rb and Cs were lost to the exomorphic halos: estimates range from 10% to 43% for Sn, 6% to 24% for Rb and 17% to 63% for Cs.

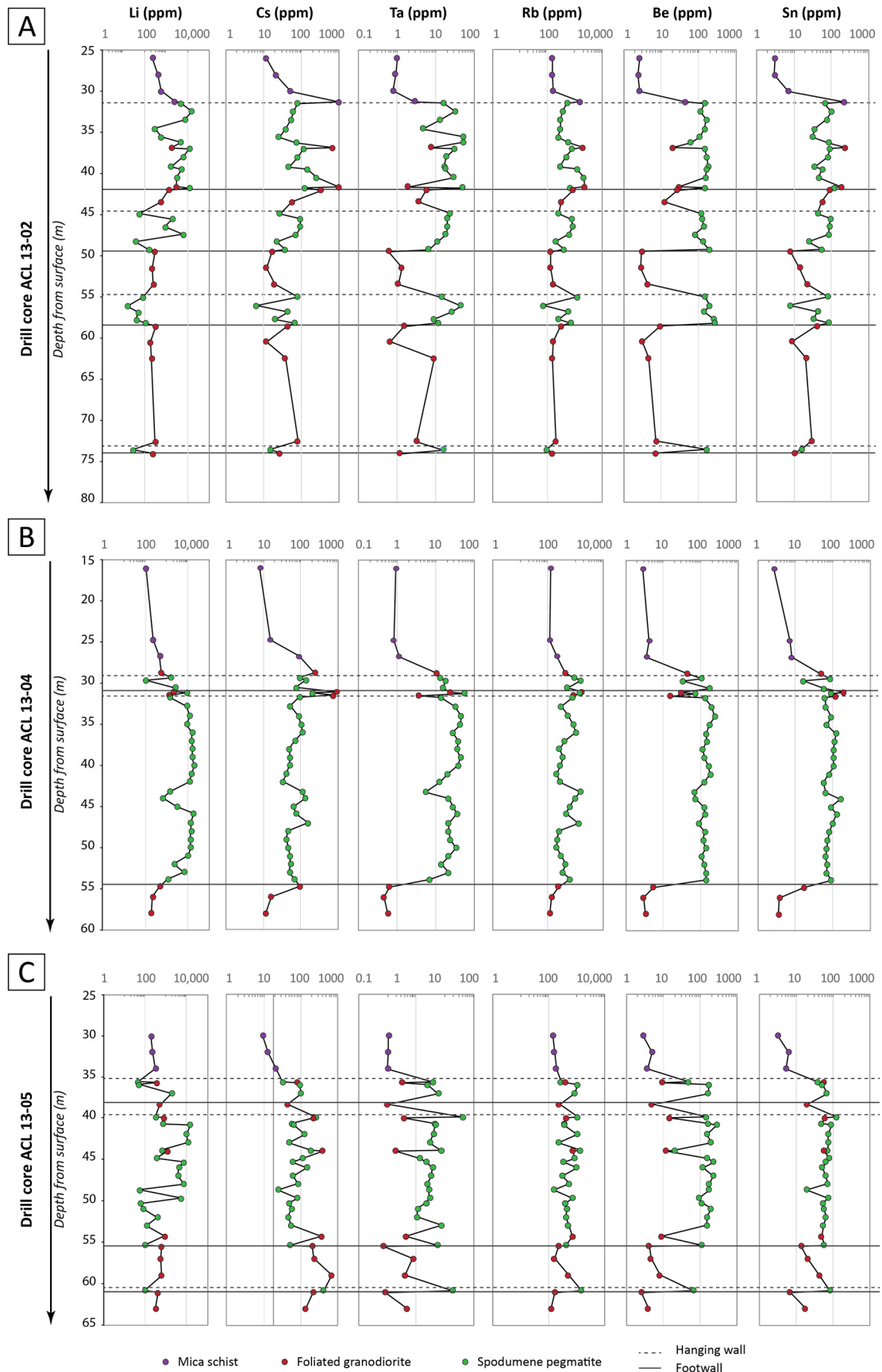


Figure 8. Geochemical profiles for Aclare drill cores (A) ACL 13-02, (B) ACL 13-04 and (C) ACL 13-05. A 30-cm-wide spodumene pegmatite intrusion is omitted in (B). Drill holes intercepted pegmatites at ~90°.

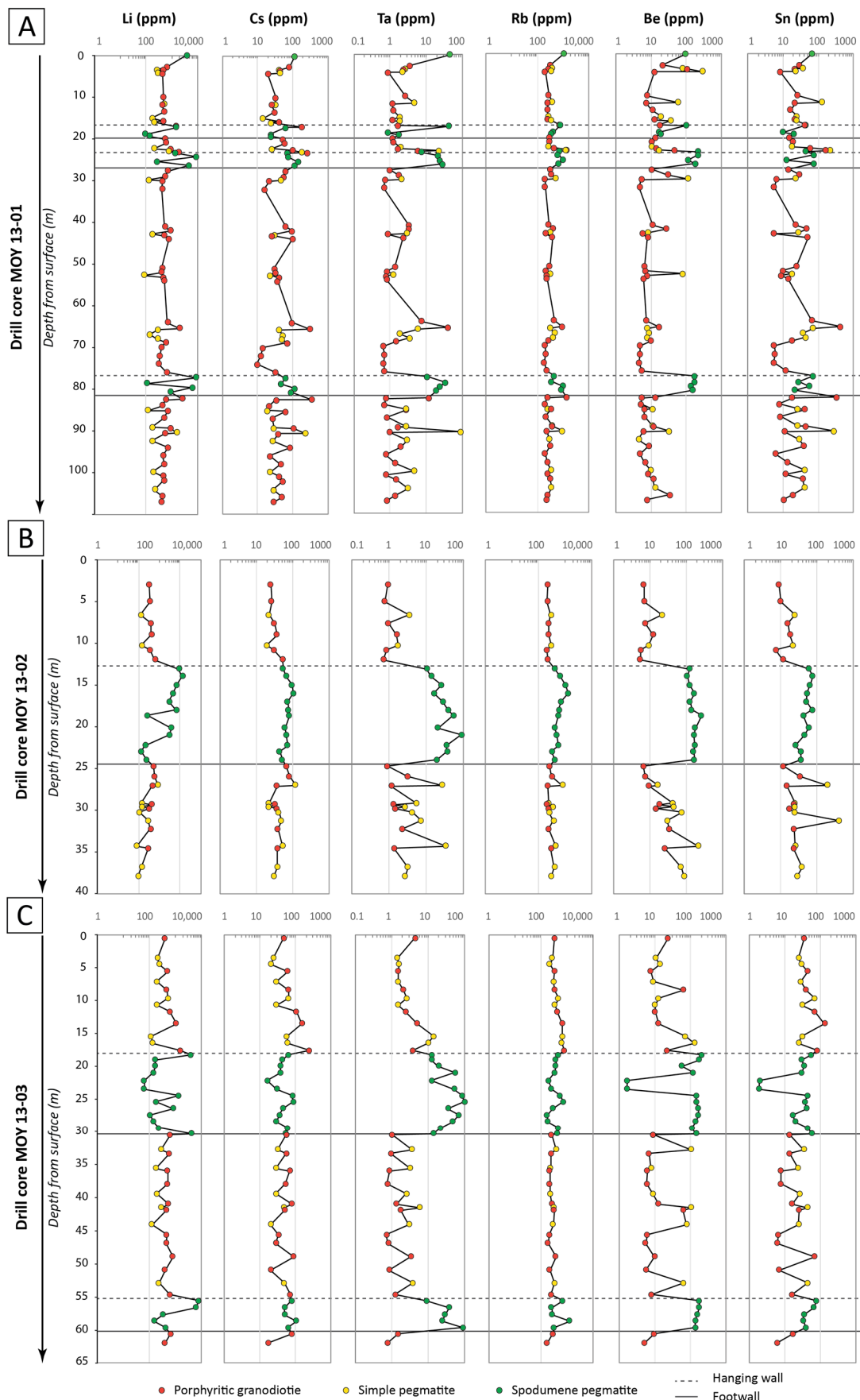


Figure 9. Geochemical profiles for Moylisha drill cores (A) MOY 13-01, (B) MOY 13-02 and (C) MOY 13-03. Drill holes intercepted pegmatites at $\sim 90^\circ$.

Table 2. Estimated mean concentrations (ppm) of key elements in the exomorphic halos, weighted by drill hole interval length.

Drill Core	Element (ppm)	Total (SP + Wall Rocks)	Total (Wall Rocks Only)	% of Element in Halo
ACL 13-02	Li	3881	189	5%
	Cs	126	48	38%
	Ta	25	2	7%
	Rb	744	103	14%
	Be	149	4	3%
	Sn	79	17	22%
ACL 13-04	Li	9840	171	2%
	Cs	129	55	43%
	Ta	27	1	3%
	Rb	672	78	12%
	Be	134	3	2%
	Sn	94	9	10%
ACL 13-05	Li	4021	134	3%
	Cs	227	144	63%
	Ta	41	2	4%
	Rb	671	78	12%
	Be	172	2	1%
	Sn	71	9	13%
MOY 13-01	Li	3501	216	6%
	Cs	109	31	28%
	Ta	23	1	3%
	Rb	758	77	10%
	Be	150	6	4%
	Sn	60	14	23%
MOY 13-02	Li	4138	113	3%
	Cs	86	14	17%
	Ta	35	1	2%
	Rb	672	41	6%
	Be	170	8	5%
	Sn	60	9	15%
MOY 13-03	Li	1503	187	12%
	Cs	100	48	48%
	Ta	43	1	3%
	Rb	563	138	24%
	Be	137	10	7%
	Sn	62	26	43%

SP = spodumene pegmatites. Totals calculated exclude background. Full detailing of calculations in Supplementary Table S2.

5. Discussion

5.1. Pegmatite–Country Rock Interactions and Exomorphic Halo Formation

The metasomatism of wall rocks has been well studied around a variety of types of granitic intrusions and related ore deposits (e.g., [38–40]). Chemical changes and often recognizable mineral assemblages are developed, mostly following an alkalic to argillic sequence that represents the increasing activity of H^+ ions in the system as it evolves to lower temperatures and pressures [6]. This process has been linked to the fracture-controlled expulsion of highly reactive hydrothermal saline and water-/vapor-rich fluids that build up during magmatic evolution [41,42]. It is not uncommon that late-stage magmatic fluids are also carriers of various elements of economic interest, so exomorphic halos and ore deposits could be frequently linked.

Wall-rock halos formed by hydrothermal alterations can range from decimeter to meter scales in Sn-W deposits (e.g., [43]) and up to kilometer scale alteration zones in porphyry deposits (e.g., [44]). Studies on halos around evolved pegmatites [8,11,12,14] have identified replacive metasomatic aureoles of a few to tens of meters into different types of host rocks, which may enclose the pegmatite body almost continuously. Concentrations of Li, Rb and Cs above the background in the metamorphosed volcanic country rock of a lithium pegmatite dike were detected up to 150 m away from the contact [45].

The crystallization of tourmaline and/or rare element-bearing micas are commonly described in lithium pegmatite wall rocks, e.g., [13,46,47]. In Leinster, the presence of tourmaline in spodumene pegmatite wall rock schists of the Ribband Group has already been described [17]. Moreover, the existence of exomorphic halos around Leinster pegmatites has previously been inferred from soil enrichment in Li, Rb, Ba, Sr, Cu, Zn, Pb and Sn above spodumene pegmatites, with concentrations up to double that in soil above more distal granitic or metasedimentary rocks [48].

Exomorphic halos identified around Leinster spodumene pegmatites in this study are characterized by enrichment in Li, Rb, Be and especially Cs, as well as the high-field-strength elements Ta and Sn, in both mica schist and granitic rocks near contacts with the pegmatites (Figure 10A). The geochemical signature of the exomorphic halos partly matches the overall signature of albitite (e.g., increased Be and Rb linked to the crystallization of beryl and siderophyllite in halos), but contrasts with the signatures of Li, Cs, Sn and Ta, which are depleted in albitite when compared to halos (e.g., Figures 6A and 7B). Halo enrichment in B can also be inferred from the formation of tourmaline in spodumene pegmatite exocontacts (e.g., Figure 5B,D,F); since tourmaline is rare in the pegmatites, it is assumed that B was present, but not saturated, throughout pegmatite crystallization [18]. It is proposed that halos are associated with albitite crystallization and were, therefore, formed after the crystallization of coarse-grained pegmatite crystals. Consequently, even though the studied drill core geochemical profiles may fail to reveal some three-dimensional variation, halo chemistry is qualitatively consistent with mineralogical and textural features in all drill cores analyzed.

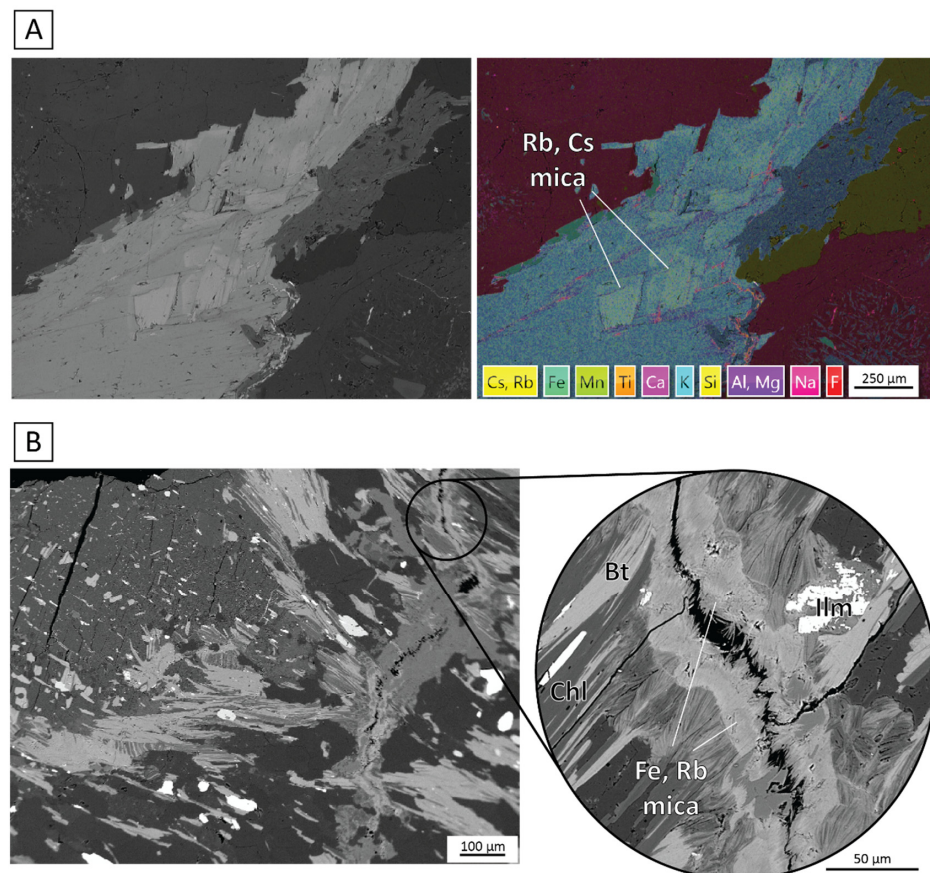


Figure 10. Example of BSE images and EDS map of halo micas showing enrichment in the elements discussed. (A) Micas in granitic wall rock enriched in Rb, Cs and probably Li (ACL 13-05). (B) Micas enriched in Fe, Rb (and probably Li), tentatively classified as siderophyllite, in fractures in the hanging wall mica schist approximately 3 m from the top of a spodumene pegmatite intersection (ACL 13-02).

With the ongoing crystallization of a pegmatite body and formation of rare-element minerals, it is expected that the residual fluid will be enriched in H₂O and fluxes that control the solubility of other incompatible elements, e.g., [19,20,49]. Considering the petrographic characteristics explored earlier, it is suggested that after a crystalline framework was formed, the H₂O- and flux-rich residual fluids from pegmatite crystallization led to its alteration through “auto-metasomatism”, in which K-feldspar and spodumene were consumed [18–20]. At some stage, a hydrothermal fluid exsolved from the residual fluid, probably as H₂O reached a saturation of ~11.5 wt % in Al-saturated melts [50], after the resorption of aluminous minerals into the fluid caused increased polymerization, and was mobilized into country rocks causing exomorphic halos. Therefore, this fluid generated in the final stages of pegmatite crystallization, in part, crystallized within the intrusion, forming the albitic late primary assemblage, and in part, was mobilized into country rocks through fracturing (Figure 10B), in agreement with a recent model of magmatic-hydrothermal transition at the end of pegmatite crystallization [19,20]. Excess Li, B, Rb and other elements in the halo-forming fluid are consistent with the absence of major phases bearing these elements in albitite. This model is supported by the consistent internal evolution of pegmatites and halo budgets among different areas and spodumene pegmatite bodies. More complex interactions and halo patterns due to multiple pegmatite pulses cannot be ruled out, but more detailed structural and geochronological characterization would be required to detect and resolve them.

Since no obvious mineralogical changes in wall rocks have been observed more than a few tens of centimeters from pegmatite contacts, micas in wall rocks are likely to be the main distal halo mineral. Micas can generally accommodate all halo elements identified, e.g., [51,52], and thus, compositions of micas crystallized in wall rocks during halo formation are likely to differ significantly from the compositions of these minerals outside halos. This has been reported in Leinster for a few of the elements [18]: Rb₂O and Cs₂O in micas in a mica schist vary from below the detection limit in distal samples (>5 m away from spodumene pegmatite contact) to up to 0.8 wt% Rb₂O and 0.4 wt% Cs₂O in exocontact samples. A systematic analysis has not yet been done for granitic country rocks, but Rb₂O and Cs₂O in exocontacts in granite are detectable at concentrations of around 0.4 wt.% and 0.15 wt.%, respectively. Individual quantitative SEM-EDS point analyses (following the method described in [19]) of dark mica in granodiorite within 1 m of the spodumene pegmatite contact at Aclare yielded up to 0.9% wt.% Rb₂O and 1.9% wt.% Cs₂O.

In Leinster, the fluid’s geochemical composition (B, H₂O) seems to have controlled the partitioning of Li, Rb, Be, Sn and Ta, and have been an cause of the especially strong partitioning of Cs, into the fluid and, consequently, to the halos, which supports some previous findings [48]. The presence of meter-scale exomorphic halos of alkali elements and fluxes is in accordance with halos described around spodumene pegmatites elsewhere [8,9,53,54]. However, evidence for the mobilization of Ta has not been previously described in pegmatite halos. It is also important to note that the percentage of elements in halos (Table 2) in this pegmatitic system can reach over 5% for Ta and Be, over 10% for Li and Rb and over 40% for Cs and Sn, which has major implications for the estimation of pegmatite starting compositions for geochemical modeling, especially when the minerals in which some of these elements are essential are absent from pegmatites, as is the case in Leinster for B and Cs. Existing pegmatite concentrations of these elements must be regarded as minimal until their potential loss to wall rocks is evaluated.

5.2. Economic Implications

Albite-spodumene pegmatites, such as those at Leinster, are economically interesting due to their typically higher Li concentrations compared to other LCT pegmatite types [30]. Soil concentrations of Li, Rb, Ta and Cs have been used to target areas for exploration in the poorly exposed Leinster belt [48]. The use of country rock chemical composition as an exploration tool for spodumene pegmatites in Leinster is shown to be another viable tool, in agreement with findings from similar studies in other evolved pegmatites, e.g., [45,55].

However, if the halo formation model proposed is realistic, the less altered pegmatite bodies will have less pronounced halos of these elements and will be harder to target, yet be potentially of a higher grade. Spodumene is the economic target mineral in Leinster and because its breakdown is related to the presence of albitite, pegmatites with well-preserved spodumene may have spatially smaller soil anomalies than pegmatites with an extensive spodumene breakdown. The possible existence of spodumene pegmatites that have lost all their spodumene by an alteration to albitite, or otherwise, must also be considered. Such intrusions might be surrounded by intense Li halos, but be of no economic interest for Li. Differences in the initial concentrations of H₂O and other fluxing elements such as B, F and P in the pegmatite-forming magma may influence the extent of the later replacement and rare-element mineral breakdown at late-stages of pegmatite crystallization. Three other factors likely to affect halo formation include depth of emplacement, expected to have a strong control on fluid escape, the mineralogy and texture of host rocks, expected to control the dimensions and density of fluid-filled fractures, and the orientation of pegmatite intrusions, with halo-forming fluids more prone to escape upwards than downwards.

The proportions of rare elements released to the halo vary from element to element and between different pegmatites. Whilst the controlling factors in these variations are not well understood, in the studied examples, a much larger proportion of Cs (over 40%) appears to be lost to the halo compared to other economically valuable elements (Li, Rb and Ta) where typically less than 20% is lost (Table 2). Unusually low levels of a late-stage alterations during the magmatic-hydrothermal transition at the end of pegmatite crystallization may, therefore, likely be the most prospective for economic Cs' concentrations in pegmatites, unless the alteration is correlated with concentrations of these elements in pegmatite magma. The possibility of economic Cs, and other element, concentrations in pegmatite halos must also be considered if the elements occur here in an economically extractable form. This, in turn, requires further detailed work on halo mineralogy, mineral chemistry and texture with a geometallurgical focus.

6. Conclusions

Unzoned to weakly zoned spodumene pegmatites in the Leinster pegmatite belt host high concentrations of Li (1.5–3% Li₂O) and are a potential source of high-technology metals such as Ta and Sn. Their predominant primary assemblage consists of spodumene + K-feldspar + albite + quartz + muscovite, and common accessory minerals include garnet, apatite and beryl. Spodumene crystals are typically present from within a few centimeters from the wall rocks to the centers of intrusions, suggesting early-stage Li-saturation. Primary minerals are often replaced by late primary fine-grained albitite, comprising albite (~90%) with accessory minerals including muscovite, garnet, apatite, beryl, cassiterite and columbite-group minerals. This sodic alteration can be restricted, occurring as isolated patches amongst primary minerals or accumulated in larger volumes with oriented albite laths, suggesting a flow structure.

Exomorphic halos were formed in both mica schists and granitic rocks adjacent to spodumene pegmatites, as evidenced by the mineralogy and geochemistry of wall rocks. Although observable mineralogical halos only extend a few to tens of centimeters, minimum exomorphic halo widths of two to five meters into country rocks are identified, presenting enrichment in Li, Rb, Be, B, Cs, Sn and Ta, a signature that, in part, compares with and, in part, contrasts with that of fine-grained albitite in spodumene pegmatites. It is suggested that after a process of auto-metasomatism, in which coarse, pegmatitic K-feldspar and spodumene were partially resorbed into residual liquid, a fluid rich in H₂O and B exsolved, leading to the partitioning of the halo elements into this fluid. Hydrothermal fluid was probably expelled into country rocks, where it formed rare-element halos, at the time of albitite crystallization. The economically relevant enrichment of rare metals in spodumene pegmatites and their halos presents challenges as well as opportunities to mineral exploration strategies.

Supplementary Materials: The following supporting information can be downloaded at: <https://www.mdpi.com/article/10.3390/min12080981/s1>, Supplementary Table S1: Results of litho geochemistry of drill cores, and Supplementary Table S2: Exomorphic halo calculations.

Author Contributions: Conceptualization, R.B. and J.F.M.; Data curation, Renata Barros; Formal analysis, R.B.; Investigation, R.B., D.K. and T.F.; Methodology, R.B., J.F.M. and J.H.; Resources, J.H.; Supervision, J.F.M. and J.H.; Visualization, R.B. and D.K.; Writing—original draft, R.B.; Writing—review and editing, D.K., J.F.M., T.F. and J.H. All authors have read and agreed to the published version of the manuscript.

Funding: This research was funded by CAPES (Coordenação de Aperfeiçoamento de Pessoal de Nível Superior), grant number 99999.009548/2013-00. This publication has emanated from research supported in part by a research grant from the Science Foundation Ireland (SFI) [grant number 13/RC/2092], co-funded under the European Regional Development Fund, and from a study funded by the European Commission's Horizon 2020 innovation program under grant agreement No 869274, project GREENPEG New Exploration Tools for European Pegmatite Green-Tech Resources.

Data Availability Statement: The data presented in this study are available in this article and its Supplementary Material.

Acknowledgments: The authors thank five anonymous reviewers who provided valuable feedback to improve this manuscript. The authors also thank two anonymous reviewers for their comments and suggestions on an earlier version of this manuscript. The authors thank Tom Culligan for making the thin sections, the staff of Aurum, especially Mark Holdstock, Graham Parkin and Emma Sheard, the staff of Blackstairs Lithium Ltd., especially Patrick McLaughlin and Gregory Sotiropoulos, and Radek Škoda and Petr Gadas from Masaryk University Brno for some of the BSE images used in the paper.

Conflicts of Interest: The authors declare no conflict of interest.

References

1. Glover, A.J.; Rogers, W.Z.; Barton, J.E. Granitic Pegmatites: Storehouses of Industrial Minerals. *Elements* **2012**, *8*, 269–273. [[CrossRef](#)]
2. Linnen, R.L.; Van Lichtenvelde, M.; Černý, P. Granitic Pegmatites as Sources of Strategic Metals. *Elements* **2012**, *8*, 275–280. [[CrossRef](#)]
3. London, D. Rare-Element Granitic Pegmatites. In *Rare Earth and Critical Elements in Ore Deposits*. Society of Economic Geologists; Verplanck, P.L., Hitzman, L.W., Eds.; Society of Economic Geologists, Inc.: Littleton, CO, USA, 2016; Volume 18, pp. 165–194.
4. United States Geological Survey. *Mineral Commodity Summaries*; United States Geological Survey: Reston, VA, USA, 2022; p. 202.
5. European Commission. *Critical Raw Materials Resilience: Charting a Path towards Greater Security and Sustainability*; European Commission: Brussels, Belgium, 2020; p. 23.
6. Pirajno, F. *Hydrothermal Processes and Mineral Systems*; Springer: Berlin/Heidelberg, Germany, 2009; p. 1250.
7. Smith, R.E.; Perdrix, J.L.; Davis, J.M. Dispersion into pisolitic laterite from the Greenbushes mineralized Sn-Ta pegmatite system, Western Australia. *J. Geochem. Explor.* **1987**, *28*, 251–265. [[CrossRef](#)]
8. Shearer, C.K.; Papike, J.J.; Simon, S.B.; Laul, J.C. Pegmatite-wallrock interactions, Black Hills, South Dakota: Interaction between pegmatite-derived fluids and quartz-mica schist wallrock. *Am. Mineral.* **1986**, *71*, 518–539.
9. Trueman, D.L.; Černý, P. Exploration for rare-element granitic pegmatites. In *Granitic Pegmatites in Science and Industry: Mineralogical Association of Canada Short Course Handbook*; Černý, P., Ed.; Mineralogical Association of Canada: Quebec, QC, Canada, 1982; Volume 8, pp. 463–493.
10. Selway, J.B.; Breaks, F.W.; Tindle, A.G. A review of rare-element (Li-Cs-Ta) pegmatite exploration techniques for the Superior Province, Canada, and large worldwide tantalum deposits. *Explor. Min. Geol.* **2005**, *14*, 1–30. [[CrossRef](#)]
11. Galeschuk, C.R.; Vanstone, P.J. Exploration for buried rare-element pegmatites in the Bernic Lake area of southeastern Manitoba. In *Rare-Element Geochemistry and Mineral Deposits, Geological Association of Canada, Short Course Notes*; Linnen, R.L., Samson, I.M., Eds.; Geological Association of Canada: St. John's, NL, Canada, 2005; Volume 17, pp. 153–167.
12. Galeschuk, C.R.; Vanstone, P.J. Exploration techniques for rare-element pegmatite in the Bird River greenstone belt, southeastern Manitoba. In *Proceedings of the Exploration 07: Fifth Decennial International Conference on Mineral Exploration*, Toronto, ON, Canada, 9–12 September 2007; Milkereit, B., Ed.; 2007; pp. 823–839.
13. Jolliff, B.; Papike, J.; Laul, J. Mineral recorders of pegmatite internal evolution: REE contents of tourmaline from the Bob Ingersoll pegmatite, South Dakota. *Geochim. Cosmochim. Acta* **1987**, *51*, 2225–2232. [[CrossRef](#)]
14. Morgan VI, G.B.; London, D. Alteration of amphibolitic wallrocks around the Tanco rare element pegmatite, Bernic Lake, Manitoba. *Am. Mineral.* **1987**, *72*, 1097–1121.

15. Fritschle, T.; Daly, J.S.; Whitehouse, M.J.; McConnell, B.; Buhre, S. Multiple intrusive phases in the Leinster Batholith, Ireland: Geochronology, isotope geochemistry and constraints on the deformation history. *J. Geol. Soc. Lond.* **2018**, *175*, 229–246. [[CrossRef](#)]
16. Luecke, W. Lithium pegmatites in the Leinster Granite (southeast Ireland). *Chem. Geol.* **1981**, *34*, 195–233. [[CrossRef](#)]
17. Whitworth, M.P. Petrogenetic implications of garnets associated with lithium pegmatites from SE Ireland. *Mineral. Mag.* **1992**, *56*, 75–83. [[CrossRef](#)]
18. Barros, R.; Kaeter, D.; Menuge, J.F.; Škoda, R. Controls on chemical evolution and rare element enrichment in crystallising albite-spodumene pegmatite and wallrocks: Constraints from mineral chemistry. *Lithos* **2019**, 352–353, 105289. [[CrossRef](#)]
19. Kaeter, D.; Barros, R.; Menuge, J.F.; Chew, D.M. The magmatic–hydrothermal transition in rare-element pegmatites from southeast Ireland: LA-ICP-MS chemical mapping of muscovite and columbite–tantalite. *Geochim. Cosmochim. Acta* **2018**, *240*, 98–130. [[CrossRef](#)]
20. Kaeter, D.; Barros, R.; Menuge, J.F. Metasomatic High Field Strength Element, Tin, and Base Metal Enrichment Processes in Lithium Pegmatites from Southeast Ireland. *Econ. Geol.* **2020**, *116*, 169–198. [[CrossRef](#)]
21. Holdsworth, R.E.; Woodcock, N.H.; Strachan, R.A. Geological framework of Britain and Ireland. In *Geological History of Britain and Ireland*, 2nd ed.; Woodcock, N.H., Strachan, R.A., Eds.; Wiley Blackwell: Chichester, UK, 2009; p. 442.
22. Chew, D.M. Grampian Orogeny. In *The Geology of Ireland*, 2nd ed.; Holland, C.H., Sanders, I., Eds.; Dunedin Academic Press: Edinburgh, UK, 2009.
23. McKerrow, W.S.; Mac Niocaill, C.; Ahlberg, P.E.; Clayton, G.; Cleal, C.J.; Eagar, M.C. The Late Palaeozoic relations between Gondwana and Laurasia. *Geol. Soc. Lond. Spec. Publ.* **2000**, *179*, 9–20. [[CrossRef](#)]
24. Tietzsch-Tyler, D.; Sleeman, A.G. *Geology of Carlow-Wexford: A Geological Description to Accompany the Bedrock Geology 1:100,000 Map Series, Sheet 19*; Geological Survey Ireland: Dublin, Ireland, 1994; p. 57.
25. McConnell, B.; Philcox, M.E. *Geology of Kildare-Wicklow: A Geological Description, with Accompanying Bedrock Geology 1:100,000 Scale Map, Sheet 16*; Geological Survey Ireland: Dublin, Ireland, 1994; p. 69.
26. Grogan, S.E.; Reavy, R.J. Disequilibrium textures in the Leinster Granite Complex, SE Ireland: Evidence for acid-acid magma mixing. *Mineral. Mag.* **2002**, *66*, 929–939. [[CrossRef](#)]
27. Chew, D.M.; Stillman, C.J. Late Caledonian orogeny and magmatism. In *The Geology of Ireland*, 2nd ed.; Holland, C.H., Sanders, I., Eds.; Dunedin Academic Press: Edinburgh, UK, 2009; pp. 143–173.
28. McArdle, P.; Kennedy, M.J. The East Carlow Deformation Zone and its regional implications. *Geol. Surv. Irel. Bull.* **1985**, *3*, 237–255.
29. Sweetman, T.M. The geology of the Blackstairs Unit of the Leinster Granite. *Ir. J. Earth Sci.* **1988**, *9*, 39–59.
30. Černý, P.; Ercit, T.S. The classification of granitic pegmatites revisited. *Can. Mineral.* **2005**, *46*, 2005–2026. [[CrossRef](#)]
31. McConnell, B.J.; Morris, J.H.; Kennan, P.S. A comparison of the Ribband Group (southeastern Ireland) to the Manx Group (Isle of Man) and Skiddaw Group (northwestern England). *Geol. Soc. Lond. Spec. Publ.* **1999**, *160*, 337–343. [[CrossRef](#)]
32. Graham, J.R.; Stillman, C.J. Ordovician of the south. In *The Geology of Ireland*, 2nd ed.; Holland, C.H., Sanders, I., Eds.; Dunedin Academic Press: Edinburgh, UK, 2009; pp. 103–117.
33. Barros, R.; Menuge, J.F. The Origin of Spodumene Pegmatites Associated with the Leinster Granite In Southeast Ireland. *Can. Mineral.* **2016**, *54*, 847–862. [[CrossRef](#)]
34. Rudnick, R.L.; Gao, S. Composition of the continental crust. In *Treatise on Geochemistry*; Rudnick, R.L., Ed.; Elsevier: Amsterdam, The Netherlands, 2003; Volume 3, pp. 1–64.
35. Lima, A.M.C. Estrutura, Mineralogia e Gênesis dos Filões Aplitopegmatíticos com Espodumena da Região Barroso-Alvão. Ph.D. Thesis, Universidade do Porto, Porto, Portugal, 2000; p. 270.
36. Groat, L.A.; Mulja, T.; Mauthner, M.H.F.; Ercit, T.S.; Raudsepp, M.; Gault, R.A.; Rollo, H.A. Geology and mineralogy of the Little Nahanni rare-element granitic pegmatites, Northwest Territories. *Can. Mineral.* **2003**, *41*, 139–160. [[CrossRef](#)]
37. London, D.; Kontak, D.J. Granitic pegmatites: Scientific wonders and economic bonanzas. *Elements* **2012**, *8*, 257–261. [[CrossRef](#)]
38. Štemprok, M.; Novák, J.K.; David, J. The association between granites and tin-tungsten mineralization in the eastern Krušné hory (Erzgebirge), Czech Republic. *Monogr. Ser. Miner. Depos.* **1994**, *37*, 97–129.
39. Li, H.; Palinkaš, L.A.; Evans, N.J.; Watanabe, K. Genesis of the Huangshaping W–Mo–Cu–Pb–Zn deposit, South China: Role of magmatic water, metasomatized fluids, and basinal brines during intra-continental extension. *Geol. J.* **2019**, *55*, 1409–1430. [[CrossRef](#)]
40. Llera, A.R.; Fuertes-Fuente, M.; Cepedal, A.; Martín-Izard, A. Barren and Li–Sn–Ta Mineralized Pegmatites from NW Spain (Central Galicia): A Comparative Study of Their Mineralogy, Geochemistry, and Wallrock Metasomatism. *Minerals* **2019**, *9*, 739. [[CrossRef](#)]
41. Burnham, C.W. Magmas and hydrothermal fluids. In *Geochemistry of Hydrothermal ore Deposits*, 3rd ed.; Barnes, H.L., Ed.; Wiley and Sons: New York, NY, USA, 1997; pp. 63–123.
42. William-Jones, A.E.; Heinrich, C.A. Vapor transport of metals and the formation of magmatic-hydrothermal ore deposits. *Econ. Geol.* **2005**, *100*, 1287–1312. [[CrossRef](#)]
43. Lecumberri-Sanchez, P.; Vieira, R.; Heinrich, C.A.; Pinto, F.; Wälle, M. Fluid-rock interaction is decisive for the formation of tungsten deposits. *Geology* **2017**, *45*, 579–582. [[CrossRef](#)]
44. Sillitoe, R.H. Porphyry Copper Systems. *Econ. Geol.* **2010**, *105*, 3–41. [[CrossRef](#)]

45. Martins, T.; Linnen, R.L.; Fedikow, M.A.F.; Singh, J. Whole-rock and mineral geochemistry as exploration tools for rare-element pegmatite in Manitoba: Examples from the Cat Lake-Winnipeg River and Wekusko Lake pegmatite fields (parts of NTS 52L6, 63J13). *Manit. Geol. Survey Rep. Act.* **2017**, *5*, 42–51.
46. Roda-Robles, E.; Pesquera, A.; Gil-Crespo, P.P.; Torres-Ruiz, J. Occurrence, paragenesis and compositional evolution of tourmaline from the Tormes Dome area, Central Iberian Zone, Spain. *Can. Mineral.* **2011**, *49*, 207–224. [[CrossRef](#)]
47. Kontak, D.J. Nature And Origin of an LCT-Suite Pegmatite with Late-Stage Sodium Enrichment, Brazil Lake, Yarmouth County, Nova Scotia. I. Geological Setting and Petrology. *Can. Mineral.* **2006**, *44*, 563–598. [[CrossRef](#)]
48. Luecke, W. Soil geochemistry above a lithium pegmatite dyke at Aclare, southeast Ireland. *Ir. J. Earth Sci.* **1984**, *6*, 205–211.
49. London, D.; Morgan, G.B., VI. The pegmatite puzzle. *Elements* **2012**, *8*, 263–268. [[CrossRef](#)]
50. London, D.; Hervig, R.L.; Morgan, G.B., VI. Melt-vapor solubilities and elemental partitioning in peraluminous granite-pegmatite systems: Experimental results with Macusani glass at 200 MPa. *Contrib. Mineral. Petrol.* **1988**, *99*, 360–373. [[CrossRef](#)]
51. Tischendorf, G.; Förster, H.J.; Gottesmann, B.; Rieder, M. True and brittle micas: Composition and solid-solution series. *Mineral. Mag.* **2007**, *71*, 285–320. [[CrossRef](#)]
52. Rosing-Schow, N.; Müller, A.; Friis, H. A Comparison of the Mica Geochemistry of the Pegmatite Fields in Southern Norway. *Can. Mineral.* **2018**, *56*, 463–488. [[CrossRef](#)]
53. Bettenay, L.F.; Partington, G.A.; Groves, D.I. Development of exploration concepts for Sn-Ta pegmatites: Use of host rock associations and alteration haloes. *West. Aust. Miner. Pet. Res. Inst. Rep.* **1985**, *13*, 171.
54. Shearer, C.K.; Papike, J.J. Pegmatite-wallrock interaction: Holmquistite-bearing amphibolite, Edison pegmatites, Black Hills, South Dakota. *Am. Mineral.* **1988**, *73*, 324–337.
55. Linnen, R.L.; Galeschuk, C.; Halden, N.M. The use of fracture minerals to define metasomatic aureoles around rare-metal pegmatites. In Proceedings of the 27th International Applied Geochemistry Symposium, Tucson, Arizona, 20–24 April 2015; p. 5.